

Growth and characterization of BIS L-alanine Strontium Nitrate single crystals

G.L. Praveena¹, T.Balu², R. Sreedevi²,

¹ Department of Physics, Govindammal Aditanar College for Women, Tiruchendur -628216, TamilNadu, India

² Department of Physics, Aditanar College of Arts & Science, Tiruchendur -628216, TamilNadu, India

Abstract: Single crystals of semiorganic material BIS L-alanine Strontium Nitrate (BLASN) of size 17 x 10 x 3 mm³ have been grown by the slow evaporation of an aqueous solution of deionized water. The crystal belongs to orthorhombic system with the space group P222. The lattice parameter values of BLASN crystal are identified using single crystal XRD studies. The crystalline perfection of the crystal have been studied by powder XRD analysis. The presence of functional groups and the protonation of ions were confirmed by Fourier transform infrared transmission (FTIR). Optical transmittance of the grown crystals have been studied by UV-vis NIR spectrum. The optical band gap of the grown crystal is 5.511 eV. Thermal stability of the crystal was investigated using thermogravimetric and differential thermal analysis. The mechanical behavior has been analyzed by Vickers microhardness test. The second harmonic generation efficiency has been studied using Kurtz powder technique.

Keywords: Crystal growth; solubility; single crystal XRD; Powder XRD; FTIR; UV-Vis- NIR; TG/DTA; Microhardness; SHG

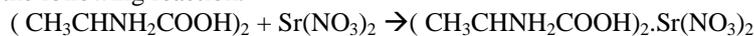
I. Introduction

The growth of high-quality nonlinear optical (NLO) materials remains a challenging endeavor for material science. Crystals of large size and with structural perfection are required for fundamental research and practical implementation in photonic and optoelectronic technology [1-3]. In this respect amino acids are interesting materials for NLO applications. Most of the natural amino acids show nonlinear optical effect. But amino acids are organic materials so they can have very large nonlinear susceptibilities relative to inorganic crystals but exhibit low damage threshold and poor processability. In recent years, efforts have been made to synthesize amino acid mixed organic inorganic complex crystals, in order to improve the chemical stability, laser damage threshold, linear and nonlinear optical properties [4-8]. Nowadays the organic and inorganic materials are being replaced by semiorganic materials because they share the properties of both organic and inorganic materials. Also semiorganic materials show large nonlinearity, low angular sensitivity and good mechanical hardness. A series of amino acid based semiorganic compounds such as L-alanine phosphoric acid, L-Valinium hydrochloride, L-isoleucinium picrate, L-arginine phosphate have been reported [9-12]. Among the amino acids, L-alanine is an acentric crystals and it is naturally occurring chiral amino acid with a non-reactive hydrophobic methyl group (CH₃) as a side chain and it is the simplest molecule having second harmonic generation (SHG) efficiency of about one third of that of the well-known KDP [13-16]. In continuation of our work on amino acid L-alanine and its complexes we are reporting for the first time the synthesis of a new nonlinear optical material bis L-alanine strontium nitrate (BLASN). In this present investigation single crystal of bis L-alanine strontium nitrate were grown from its aqueous solution by slow evaporation method. The grown crystals were characterized by single crystal XRD, Powder XRD, FTIR, UV- Vis- NIR, Microhardness, SHG.

II. Experimental Section

2.1 Synthesis

The starting material was synthesized by taking L-alanine (Merck) and strontium nitrate (Merck) in 2:1 stoichiometric ratio. The required amount of starting materials for the synthesis of BLASN salt is calculated according to the following reaction.



The calculated amount of L-alanine was first dissolved in deionized water and then strontium nitrate is added to the solution slowly by stirring. The prepared solution is first heated to 50°C and then allowed to dry at room temperature and then the salt is obtained by slow evaporation technique. The purity of the synthesized salt is further improved by successive recrystallization process.

2.2 Solubility

Solubility study was performed using a hot-plate magnetic stirrer and a digital thermometer by gravimetric method [17]. Fig.1 shows that the solubility of BLASN sample in water increases linearly with

temperature, exhibiting a high solubility gradient and positive temperature coefficient, which reveals the fact that slow evaporation technique is the appropriate method to grow single crystal of BLASN.

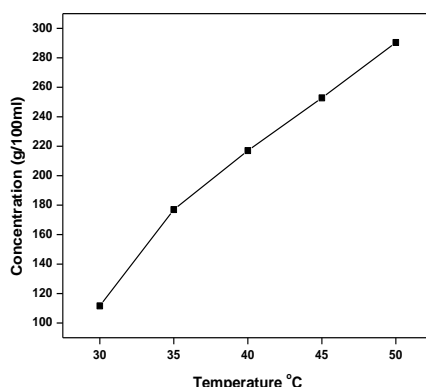


Fig 1. Solubility curve of BLASN crystal

2.2 Crystal growth

Single crystals of BLASN were grown by solution method with slow solvent evaporation technique at room temperature (30°C). In accordance with the solubility data, saturated solution of the twice re-crystallized salt of BLASN was prepared by dissolving the salt in de-ionized water by continuous stirring of the solution and filtered using 4 micro Whatmann filter paper. Then the filtered solution was taken in a beaker and covered by a perforated cover for controlled evaporation. The seed crystals of BLASN were obtained by spontaneous nucleation. Two or three good quality seed crystals of BLASN were placed in the supersaturated solution and the solution was allowed to evaporate the solvent slowly into atmosphere. A typical single crystal with size 17 x 10 x 3 mm³ was obtained within a period of 25-28 days. The grown crystal is shown in Fig.2 and the grown crystals are found to be stable, non-hygroscopic at ambient temperature, transparent and colorless.



Fig 2. As grown crystal of BLASN

III. Results and Discussion

3.1 Single Crystal XRD studies

In order to confirm the cell parameters of the grown BLASN crystals, the sample was subjected to single crystal XRD studies. The single crystal XRD study of BLASN was carried out using ENRAF NONIUS CAD4 single X-ray diffractometer with MoK_α (λ=0.71069 Å) radiation. Reflections from a finite number of planes were collected. The study revealed that grown BLASN crystal belongs to orthorhombic system with the following cell parameters a = 6.785 Å, b = 7.420 Å, c = 11.637 Å and α=β=γ= 90°

TABLE 1: Single crystal XRD data for BLASN crystal

Diffractometer	ENRAF NONIUS CAD-4
Radiation, wavelength	MoK _α , 0.71069 Å
Refinement method	Full matrix Least square method
Molecular weight	389.81 g/mol
Symmetry	Orthorhombic
Space group	P222
a	6.785 Å
b	7.420 Å

c	11.637 Å
α	90°
β	90°
γ	90°
Volume	585.86 Å ³
Z	4

3.2 Powder X-ray diffraction

Powder X-ray diffraction studies were carried out using Reich Siefert X-ray diffractometer employing $\text{CuK}\alpha$ radiation, scanning angle ranging from 10 to 80°C at a scan rate of 1°/min to study the crystallinity of the grown crystal. The various planes of reflections were indexed using indexing software and the diffraction peaks were observed. The sharp peaks confirm that the crystallinity of the grown crystal is good. This has been given in Fig.3.

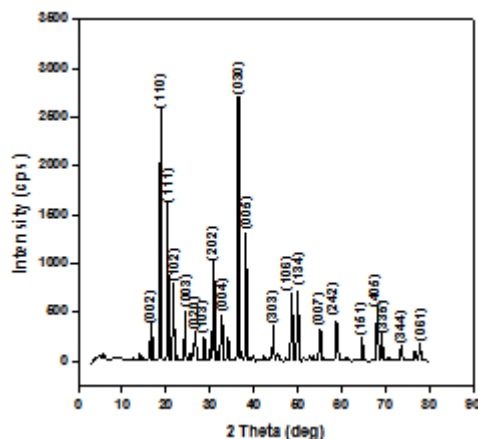


Fig 3. Powder XRD spectrum

3.3 FTIR analysis

The FTIR spectrum was recorded using a Bruker FTIR spectrometer by KBr pellet technique in the range 400–4000 cm^{-1} at room temperature. The recorded FTIR spectrum of BLASN is shown in Fig.4. The NH_2 group of L-alanine is protonated by the COOH group, giving rise to NH_3^+ and COO^- groups. Amino group absorption bands were noted at 3088.08 cm^{-1} (asymmetric stretching), 2599.65 cm^{-1} (symmetric stretching), 1619.18 cm^{-1} (asymmetric bending) and 1108.68 cm^{-1} (rocking). These bands are due to NH_3^+ ions [18]. The sharp peaks at 2293.24, 2248.94 and 2111.79 cm^{-1} are due to the combination of NH_3^+ asymmetric stretching and its torsional oscillation. The zwitterionic nature of the amino acid was evident from NH_3^+ absorption band and also the COO^- absorption peaks at 1413.85 cm^{-1} (COO^- symmetric stretching), 647.64 cm^{-1} (COO^- scissoring) and 407.64 cm^{-1} (COO^- rocking) [19,20]. A fairly strong symmetrical bending band was observed at 1508.72 cm^{-1} . The peaks observed at 1360.76 cm^{-1} was attributed to C-C stretching vibration. The peaks observed at 1302.76, 1151.20 and 1010.64 cm^{-1} are due to CH_3 symmetric wagging and rocking mode. The absorption peaks at 918.22 and 847.27 cm^{-1} are assigned to C-C-N symmetric stretching vibrations. The COO^- bending and rocking frequencies occur in the normal positions at 772.43, 722.73, 537.99 cm^{-1} . These vibrations prove the presence of expected functional groups in the compound.

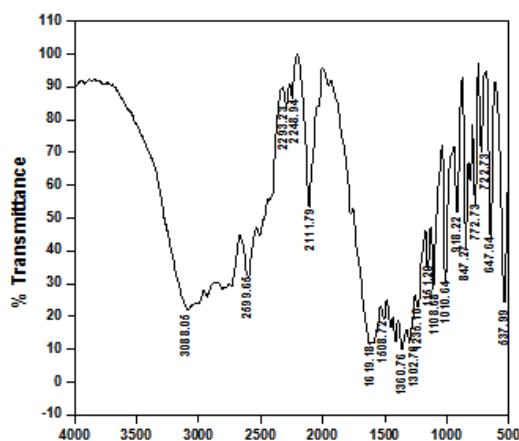


Fig 4. FTIR spectrum

3.4 UV-vis NIR analysis

A higher optical transmittance is very desirable in an NLO crystal. Optical transmission spectra were recorded using a double beam spectrophotometer in the wavelength region 190-1100 nm and the recorded spectrum is shown in Fig. 6. From the figure it is observed that the crystal shows good transmission in the entire visible and IR regions. The lower UV cut off wavelength is at 225 nm. The transmittance of BLASN increases to 93%. The improvement in the percentage of transmission may be attributed to the reduction of scattering from point and line defects in the crystal [21]. The absence of absorption of light in the visible region is an intrinsic property of all amino acids [22,23]. Absence of absorption in the region between 220 nm and 1100 nm shows that this crystal could be used for optical window applications.

The optical absorption coefficient (α) was calculated from the transmittance using the following relation.

$$\alpha = \frac{1}{t} \log\left(\frac{1}{T}\right)$$

where T is the transmittance and t is the thickness of the crystal.

Owing to the direct band gap, the crystal under study has an absorption coefficient (α) obeying the following relation for high photon energies (hv):

$$\alpha = \frac{A \sqrt{(h\nu - E_g)}}{h\nu}$$

where E_g is the optical band gap of the crystal and A is a constant. The plot of variation of $(\alpha h\nu)^{1/2}$ vs. $h\nu$ is shown in Fig. 6. E_g is evaluated by the extrapolation of the linear part [24]. The band gap is found to be 5.02eV. As a consequence of wide band gap, the grown crystal has large transmittance in the visible region [25].

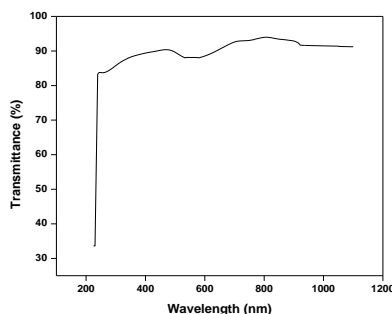


Fig 5. UV-visible transmittance spectrum

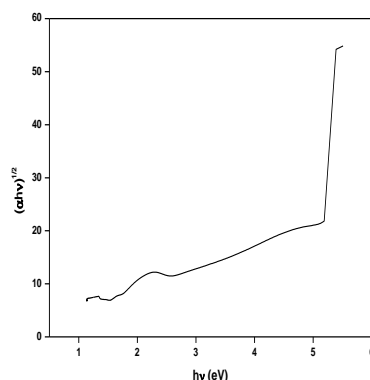


Fig 6. Plot of $(\alpha h\nu)^{1/2}$ vs photon energy

3.5 Thermal analysis

The thermogravimetric and differential thermal analysis give information regarding phase transition, water of crystallization and different stages of decomposition of the crystal [26]. The Thermogravimetric analysis (TGA) and differential thermal analysis (DTA) of the crystal was done using Perkin Elmer Diamond TGA /DTA equipment at a heating rate of 10°C / min for a temperature range of 38-549°C and the thermogram is shown in Fig.7. The TGA curve shows that the crystal is thermally stable up to 217°C and the weight loss starts above this temperature. In DTA curve a sharp endotherm observed at 266°C., is assigned to the melting

point of the specimen. The sharpness of the endothermic peak observed in DTA shows good degree of crystallinity [27] of the crystal.

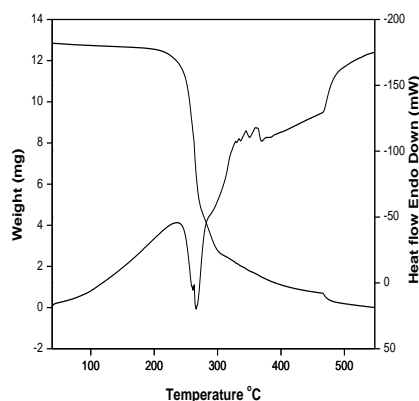


Fig 7 .TG/DTA spectrum

3.6 Evaluation of microhardness, yield strength and stiffness constant.

The mechanical properties such as hardness, yield strength and stiffness constant of crystals can be evaluated by Vickers hardness test. The hardness of a material depends on different parameters such as lattice energy, Debye temperature, heat of formation and interatomic spacing [28]. According to Gong [29], during an indentation process, the external work applied by the indenter is converted to strain energy component which is proportional to the volume of the resultant impression and the surface energy component proportional to the area of the resultant impression. Microhardness is a general microprobe technique for assessing the bond strength, apart being a measure of bulk strength. It is a measure of the material's resistance to local deformation caused by scattering or by indentation [30]. Microhardness studies were carried out using Vicker's hardness tester (LEITZ WETZLER) fitted with a diamond pyramidal indenter. It plays a key role in device fabrication. Single crystals of BLASN were used for this study. Before indentations, the crystals were carefully lapped and washed to avoid surface effects, which influence the hardness values. Indentations were made using a Vickers pyramidal indenter for various loads from 25 to 100 g. The distance between two indentation points were more than three times the diagonal length, in order to avoid any mutual interference of indentations. The measurements of the diagonal length was made at room temperature and the indentation time was 5s. The Vickers hardness number of the crystal was calculated using the relation

$$H_v = 1.8544 (P/d^2) \text{ kg/mm}^2$$

where H_v is the Vickers hardness number, P is the applied load in kg and d is the average diagonal length of the impression in mm. Measurement of hardness is a useful non destructive testing method used to determine the applicability of the crystal in the device fabrication. A plot between the hardness number and the load is depicted in Fig. 8. On further increase of the load beyond 100 g, cracks developed on the surface of the crystal. It may be due to the release of internal stress generated locally by indentation. The relation connecting the applied load and diagonal length 'd' of the indenter is given by Meyer's law [31]

$$P = kd^n$$

where n is the Meyer's index or work hardening coefficient and d is the measure of indentation size effect (ISE) and k is the material's constant. The simplest way to describe the ISE is Meyer's law. For the normal ISE behavior, the exponent $n < 1.6$. When $n > 1.6$, there is the reverse ISE behavior. When $n=1.6$, the hardness is independent of the applied test load, and is given by Kick's law [32,33]. From careful observations on various materials, Onistch [34] and Hanneman pointed out that n lies between 1 and 1.6 for moderately hard materials and it is more than 1.6 for soft materials. The value of n obtained for BLASN is 4.08 and is calculated from the plot of $\log P$ vs $\log d$ (Fig. 9), the material belongs to soft category and is in agreement with the reverse indentation size effect. Large value of n indicates large effect of dislocations [35]. An increase in the mechanical strength will have a significant effect on fabrication and processing, such as, ease of polishing and less wastage due to cracking / breakage while polishing.

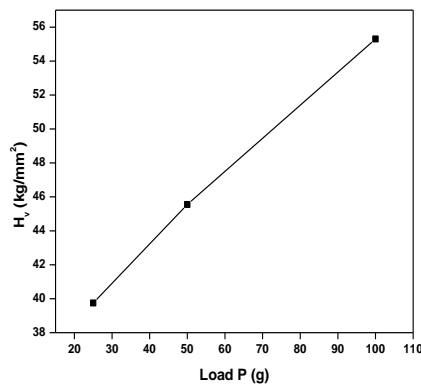


Fig 8. Plot of H_v vs load P

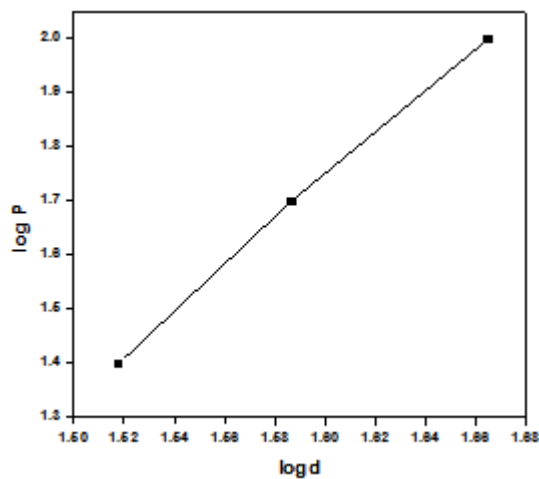


Fig 9. Plot of log P vs log d

From the hardness value, the yield strength σ_v can be calculated. The yield strength is defined as the stress at which a predetermined amount of permanent deformation occurs and it is found using the relation $(\sigma_v) = (H_v/3)$ where H_v is the hardness of the material. The load dependent of yield strength of BLASN crystal is presented in the Fig 10. It is observed that yield strength increases with increase of load and hence the grown crystal has relatively high mechanical strength. The elastic stiffness constant (C_{11}) for different loads was calculated using Wooster's empirical formula $C_{11} = H_v^{7/4}$ [36] and the variation of C_{11} with the load is depicted in Fig 11. Stiffness constant gives an idea about the tightness of bonding between neighboring atoms. From the figure 11, it is observed that the stiffness constant increases with increase of load and the high values of C_{11} indicate that the binding forces between the ions in the BLASN crystal is strong.

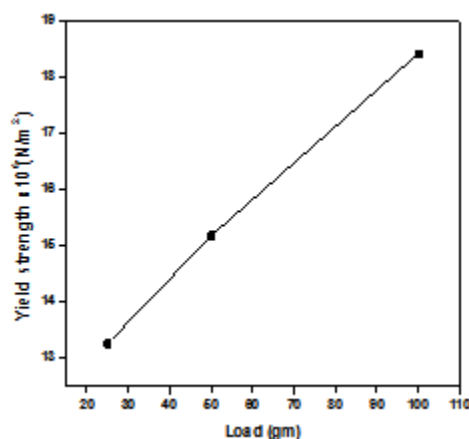


Fig 10. Variation of yield strength with the applied load

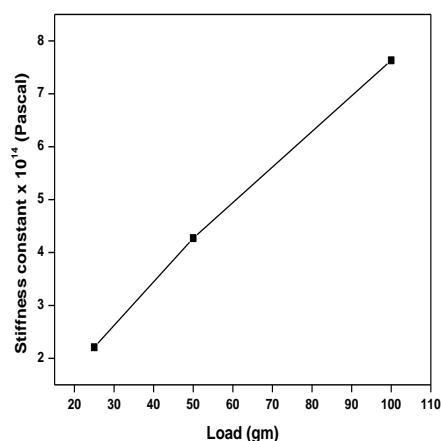


Fig 11. Variation of stiffness constant with the applied load

3.7 Second harmonic generation (SHG) studies

The second harmonic generation behavior of the powdered material was tested using the Kurtz and Perry method [37]. The crystal was illuminated using Spectra Physics Quanta Ray DHS2. Nd:YAG laser using the first harmonics output of 1064 nm with pulse width of 8ns and repetition rate 10 Hz. The second harmonics signal, generated in the crystal was confirmed from the emission of green radiation by the crystal. The SHG radiations of 532 nm green light was collected by a photomultiplier tube (PMT-HamasuR2059) after being monochromated (monochromator-Czerny-Turner) to collect only 532 nm radiation. The optical signal incident on the PMT was converted into voltage output at the CRO (Tektronix-TDS 3052B). Powdered SHG measurements using 1064 nm radiation revealed that BLASN showed SHG efficiencies 0.5 times of KDP. The SHG efficiency will vary with the particle size of the powder sample [38].

IV. Conclusion

Optical quality single crystals of semiorganic BLASN have been grown using slow evaporation solution growth technique. The grown crystals are observed to be transparent and colorless with well defined edges. The unit cell parameter values show that the crystal belongs to orthorhombic system with non centrosymmetric space group P222. The crystalline perfection of the crystal has been confirmed by powder XRD analysis. FTIR spectral analysis confirms the presence of the functional groups in the grown crystal. Optical studies show that the crystal has wide transmission range with UV cut-off wave length at 225 nm. The optical band gap energy (E_g) is found to be 5.02 eV. The thermal studies reveal that the crystal is stable up to 217°C. Hardness measurement shows that the crystal is mechanically stable up to 100 gm and increase in the work hardening coefficient may be due to the dislocation motion. The SHG efficiency of the grown crystal is found to be 0.5 times that of KDP.

Acknowledgement

The author acknowledges SAIF, IIT, Chennai for single crystal XRD analysis, STIC Cochin for FTIR, UV-vis, TGA-DTA analysis, Crescent Engineering college Chennai for SHG measurement, St. Joseph's college Trichy for microhardness measurement and the management of Govindammal Aditanar College for the support and encouragement throughout this work.

References

- [1]. M.H. Jiang, Fang, *Advanced Materials* (Weinheim, Germany) 13 (1999) 1147.
- [2]. P.N. Prasad, D.J. Williams, in: *Introduction to Nonlinear Effects in Molecules and Polymers*, Wiley, New York, 1991.
- [3]. D.S. Chemla, J. Zyss (Eds.), *Nonlinear Optical Properties of Organic Molecules and Crystals*, Academic press, New York, 1987.
- [4]. T. Pal, T. Kar, X.Q. Wang, G.Y. Zhou, D. Wang, X.F. Chen, Z.H. Yang, *J. Cryst. Growth* 235 (2002) 523.
- [5]. T. Pal, T. Kar, G. Bocelli, L. Rigi, *Cryst. Growth Des.* 3 (2003) 13.
- [6]. R.M. Kumar, D. Rajanbabu, D. Jayaraman, R. Jayavel, K.J. Kitamura, *J. Cryst. Growth* 275 (2005) 1935.
- [7]. A. Kandasamy, R. Siddeswaran, P. Murugakoothan, P.S. Kumar, R. Mohan, *Cryst. Growth Des.* 7 (2007) 183.
- [8]. K. Sethuraman, R. Ramesh Babu, R. Gopala Krishnan, P. Ramasamy, *Cryst. Growth Des.* 6 (2008) 1863.
- [9]. A.S.J. Lucia Rose, P. Selvarajan, S. Perumal, *Spectrochimica Acta part A* 81(2011) 270-275.
- [10]. Sweta Moutra, Saikat Kumar Seth, Tanusree Kar, *Journal of crystal growth* 312 (2010)
- [11]. G. Ramasamy, Subbiah Meenakshisundaram, *Optik* 125 (2014) 4422-4426.
- [12]. D. Eimerl, S. Velsko, L. Davis, F. Wang, G. Loiacono, G. Kennedy. *IEEEJ. Quantum Electron* 25 (1989) 179-193.
- [13]. Thenneti Raghavulu, G. Ramesh Kumar, S. Gokul Raj, V. Mathivanan, R. Mohan, *J. Cryst. Growth* 307 (2007) 112-115.
- [14]. M. Diem, P.L. Polavarapu, M. Oboodi, L.A. Nafie, *J. Am. Chem. Soc.* 104 (1982) 3329-3336.

- [15]. C.Razzetti, M.Ardoido, L.Zanotti, M.Zha, C.Parorici, *Cryst.Res, Technol*, 37 (2002) 456- 465.
- [16]. R.Mohan Kumar, D.Rajan Balu, D.Jayaraman, R.Jayavel, K.Kitamura, *J.Cryst. Growth* 275 (2005) e1935-e1939.
- [17]. W.S.Wang, K.Sutter, Ch.Bosshard, Z.Plan, H.Arend, P.Gunter, G.Chapius, F.Nicolo, *J.Jpn Appl. Phys.* 27 (1998) 1138.
- [18]. J. Baran, A.J. Barnes, H. Ratajczak, *Spectrochim. Acta* 51 (1995) 197-214.
- [19]. Masamichi Tsuboi, Tadao Takenishi, Asao Nakamuba, *Spectrochim. Acta* 15 (1963) 271- 284.
- [20]. F.F. Bentley, E.F. Wolfarth, *Spectrochim. Acta* 15 (1959) 165-205.
- [21]. M. Senthil Pandian, N. Pattanaboonmee, P.Ramasamy, P. Manyum, *Journal of Crystal Growth* 314 (2011) 207.
- [22]. M. Senthil Pandian, P. Ramasamy, *Journal of Crystal Growth* 312 (2010) 413.
- [23]. I.M. Pritula, Yu.N. Veliknov, *Proceedings of SPIE* 202 (1993) 3793.
- [24]. A.K. Chawla, D. Kaur, R. Chandra, *Optical Mater.* 29 (2007) 995.
- [25]. D.D.O. Eya, A.J. Ekpunobi, C.E. Okeke, *Academic Open Internet J.* 17 (2006).
- [26]. S. Janarthanan, R. Sugaraj Samuel, Y.C. Rajan, P. Suresh, K. Thangaraj, *Spectrochimica Acta Part A: Molecular and Biomolecular Spectroscopy* 105 (2013) 34-37.
- [27]. N. Vijayan, K. Nagarajan, Alex M.Z. Slawin, C. K. Shashidharan Nair, G. Bhagavannarayana, *Crystal Growth and Design* 7 (2007) 445-448.
- [28]. S. Dinakaran, S. Jerome Das, *Journal of Crystal Growth* 310 (2008) 410-413.
- [29]. J. Gong,,J. *Material science Letters* 19 (2000) 515.
- [30]. B.W. Mott, *Micro-indentation Hardness Testing*, Butterworths Publications Ltd, London, 1956, 9-21.
- [31]. E. Meyer, *Z. Phys.* 9 (1908) 66-74
- [32]. D. Tabor, *The Hardness of Metals*, Clarendon Press, Oxford, UK, (1951) 49-116.
- [33]. Yu.S. Boyarskaya, *Deformation of Crystals under Microhardness Testing Chisinau, "Shtiintsa"* 233 (1972).
- [34]. E.M. Onitsh, *Uber die Mikroharte der Metalle, Mikroskopie* 2 (1947) 131.
- [35]. S.J. Das, R. Gopinathan, *Crystal Research and Technology*, 21(1) (1992) K17.
- [36]. W.A. Wooster, *Physical properties and atomic arrangements in crystals, Rep. Prog. Phys.* 16 (1953) 62-82.
- [37]. S.K. Kurtz, T.T. Perry, *Journal of Applied Physics* 39 (1968) 3798.
- [38]. Urit Charoen-In, P.Ramasamy, P. Manyum, *Journal of Crystal Growth* 362 (2013) 220-226.